

## **Environmental Flight Acceptance Tests of the Small Earth Observation Satellite Flying Laptop**

Michael Lengowski, Fabian Steinmetz, Nico Bucher, Kai Klemich, Mark Lützner, Sabine Klinkner  
Institute of Space Systems, University of Stuttgart  
Pfaffenwaldring 29, 70569 Stuttgart, Germany, +49 711 685 69607  
lengowski@irs.uni-stuttgart.de

Eugen Mikulz  
Institute of Space Systems, German Aerospace Center  
Robert-Hooke-Str. 7, 28359 Bremen, +49 421 24420 1308  
eugen.mikulz@dlr.de

Steffen Babben  
Institute of Optical Sensor Systems, German Aerospace Center  
Rutherfordstraße 2, 12487 Berlin-Adlershof, +49 30 67055 603  
steffen.babben@dlr.de

Jens Eickhoff, Hubert Stiehle, Christoph Jean  
Airbus Defence and Space GmbH  
88039 Friedrichshafen, +49 7545 8 4178  
jens.eickhoff@airbus.com

### **ABSTRACT**

Since mid-2014, the fully integrated small satellite Flying Laptop is in the system testing phase at the Institute of Space Systems located at the University of Stuttgart in Germany. The satellite's mass is 120 kg and it is designed to conduct multi-spectral earth observation as well as to demonstrate new technologies. A part of the acceptance tests prior to launch is the environmental testing in order to verify spacecraft functionality under environmental conditions during launch and in orbit. The following three main environmental tests were successfully conducted:

- Tests of Electromagnetic Compatibility (EMC):  
The EMC test of the Flying Laptop covered the verification of electromagnetic compatibility as well as interference of the various electromagnetic signals generated on-board.
- Vibration test:  
For the structural acceptance of the spacecraft sine and random vibration tests were performed for each satellite axis.
- Thermal Balance / Thermal Vacuum test:  
The thermal vacuum test was conducted to verify the functionality of the entire satellite at hot and cold temperatures. A similar test setup was used to perform the thermal balance test that allowed the validation of the thermal model.

The environmental test campaign was completed successfully in December 2014. All system requirements were met according to the defined specifications.

### **INTRODUCTION**

The Flying Laptop is the first satellite of the Institute of Space Systems of the University of Stuttgart (Figure 1). The small satellite with its size of 600 x 700 x 870 mm<sup>3</sup> and its mass of 120 kg has been developed and built mostly by students at the university and will be

operated from an on-site ground station. The main mission goals of the spacecraft are the demonstration of innovative technologies and multi-spectral earth observation. The Flying Laptop is equipped with an experimental laser link terminal built by the German Aerospace Center (DLR), an experimental data downlink system which was developed in-house,



**Figure 1: Artist's Impression of the Satellite Flying Laptop**

and a LEON3FT based on-board computer. Furthermore, two optical camera systems and a DLR receiver for ship tracking (AIS system) serve the scientific goals of the satellite. As launch orbit a sun synchronous orbit with a local time of 9:00 to 12:00 and an altitude below 650 km is aspired. The altitude requirement results from the pursued compliance with the European Code of Conduct for Space Debris Mitigation (ref. 1). In order to re-enter on Earth within the required 25 years after end of mission the satellite shall increase its aerodynamic drag by means of a deorbit sail. Currently the flight software of the Flying Laptop is being finalized and the last functional system tests will be prepared and executed. Thus, by the end of 2015 the satellite will be completed.

The assembly, integration and test phase of the Flying Laptop started in the beginning of 2014 after the successful completion of the flatsat tests of the spacecraft's bus components verifying the correct interaction of components and software before integration into the satellite structure. Parallel to the integration of the satellite the payload flatsat tests were performed. After the end of the spacecraft integration in the middle of 2014 the system test phase began. In the environmental verification the satellite system was tested under conditions that occur throughout the mission of the spacecraft. Three environmental tests were executed on the flight hardware of the complete spacecraft: the Electromagnetic Compatibility (EMC) test, the vibration test, and the Thermal Balance / Thermal Vacuum Test. The development, the execution, as well as the results of these environmental tests will be described in the following.

### **TEST PHILOSOPHY**

In order to keep costs low the Flying Laptop was developed using a so called proto-flight approach.

Usually two models of a satellite are built, one engineering qualification model for testing and qualification, and one flight model which undergoes only flight acceptance tests. However, for the Flying Laptop only one proto-flight model was built for the satellite structure. This proto-flight model is used both for qualification tests as well as acceptance tests. Combining both models saves costs in development, material and components, but increases the risk of damaging the flight model during tests.

The overall test strategy for the Flying Laptop is to have a lean and efficient testing, that is oriented towards the mission objectives. It is distinguished between three basic types of system tests: non-functional tests, functional tests, and environmental tests. All tests aimed at the determination of satellite properties like the measurement of the satellite mass or the center of gravity are designated as non-functional tests. Functional tests focus on the verification of functional requirements and are also included in the environmental tests. Environmental tests focus on three main topics: Electromagnetic compatibility, mechanical resilience, thermal verification. Electromagnetic compatibility is required for confidence in the compatibility of the systems internal and external components, i.e. the internal harness or external communication antennas. Mechanical resilience means to demonstrate that the Flying Laptop is capable of withstanding the exposure to vibrational loads during launch. And finally, the knowledge of thermal properties is required in order to tune thermal balance points for the thermal extremes by adjusting radiators or insulation and to validate thermal simulations. All of these tests require a representative model of the satellite or the proto-flight model itself in order to guarantee maximum resemblance and therefore deliver the required confidence in the system.

## EMC TEST AT AIRBUS DEFENCE AND SPACE

The electromagnetic compatibility tests were conducted at the facility of Airbus Defence and Space (Friedrichshafen, Lake Constance, Germany) and are further described here below and in ref. 2.

### EMC Test Definition

In order to shield all tests from electromagnetic interference the Flying Laptop was placed inside an anechoic isolation chamber which can be seen in Figure 2.

Mainly four types of tests were performed:

1. Transmitter intermodulation products analysis
2. Determination of electromagnetic susceptibility of the system
3. Measurement of conducted emissions for the internal harness
4. Measurement of radiated emissions in the near field of the satellite

In the transmitter intermodulation products test the purity of the generated radio frequency signals for each rf-active on-board-component was measured. Each radio transmitter produces the final radio frequency by mixing the baseband signal with an intermediate frequency. In this process undesired byproducts are generated, i.e. sum and difference frequencies, which are normally filtered out. In this test the quality of these filters for each on-board transmitter was examined and the radiated energy resulting from intermodulation products was measured. If undetected, such byproducts can lead to severe interference on frequency bands of other components which would normally be overlooked if only one active component is considered.

### EMC Test Results

Figure 3 shows the main transmitter S-band carrier wave. Intermodulation products or spectral impurities were found neither in the near frequency range of the transmitting signal, nor in the far range. With these results the test were considered successful, meaning the quality of the intermodulation product suppression is sufficient.

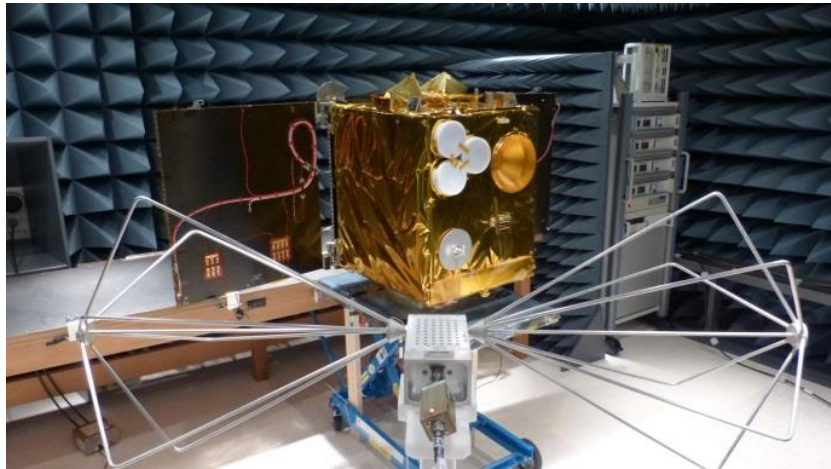


**Figure 2: Flying Laptop Spacecraft Inside Anechoic Electromagnetic Isolation Chamber at Airbus DS, Friedrichshafen**

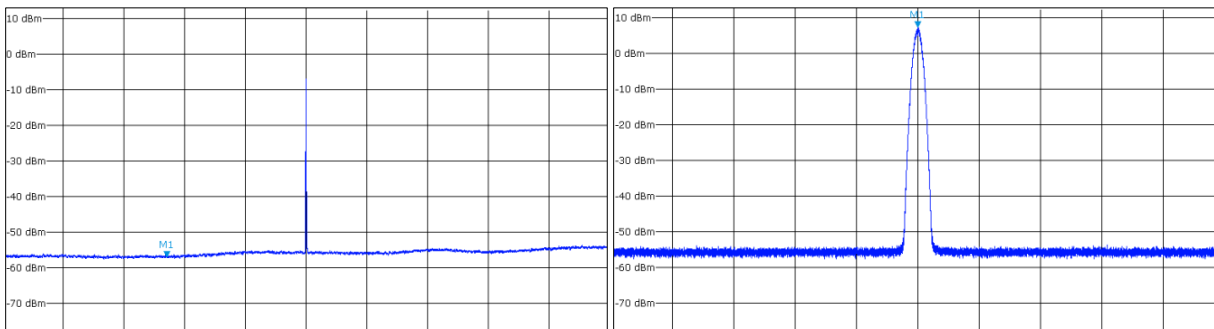


**Figure 3: Results for the Transmitter Intermodulation Products Test**

The Flying Laptop uses GPS receivers as part of its attitude control system. During the development concerns arose that radiated emissions interfere with the GPS signal reception. Therefore, one of the main targets of the electromagnetic susceptibility test was to demonstrate that GPS reception is not disturbed by the system itself or other on-board transmitters. Since one of the two antennas for S-band downlink is mounted close to the GPS antennas on the satellite's solar panel side the main focus laid on the interference of both of these antennas. A special pre-test was conducted with both antennas mounted on an aluminum plate within the anechoic chamber as shown in Figure 5. A test signal was fed into the S-band antenna and the output level was measured on the GPS antenna side. The goal was to determine if the signal amplifier behind the GPS antenna can be saturated by the incoming signal. The test was successful and showed there is enough headroom to prevent the saturation of the GPS amplifier due to downlink activity. The attenuation between the two antennas is 51 dB which leaves a safety margin of 9.5 dB before the GPS amplifier will reach its 1 dB compression point that was used to define the level for saturation.

Conducted emissions were measured using a sniffer probe on the plus pole of the power line to the spacecraft which was additionally decoupled using line impedance stabilization, see Figure 4. The main objective for this test was to provide confidence in the shielding of the internal harness and in the electrical design of the components so that crosstalk between lines is kept at an acceptable level. The conducted emissions test was performed with and without the spacecraft battery connected. In both cases the complete

system including all on-board components and payloads was activated to produce the maximum amount of emissions. Results showed that emissions on the power line are significantly lower if the internal battery is connected because it acts as a capacitor.

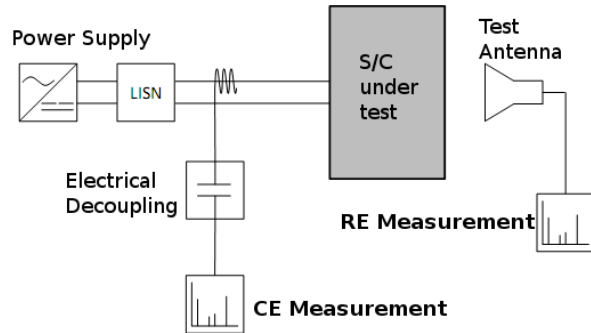


**Figure 4: Test Setup for Conducted (CE) and Radiated Emission (RE) Tests**

For the radiated emissions test the whole spectrum of radiated emissions was recorded throughout different operational states of the satellite in order to identify which components are generating typical emission patterns. Additionally, notch regions in the frequency spectrum were defined for critical frequency bands of the on-board receivers. The notch regions represent areas of interest which were examined for intrusive spurious emissions. No critical spurious emissions were found within the notch regions and the overall emission spectrum, especially in the more critical higher frequencies, were below the required limit (Figure 6 and Figure 7).

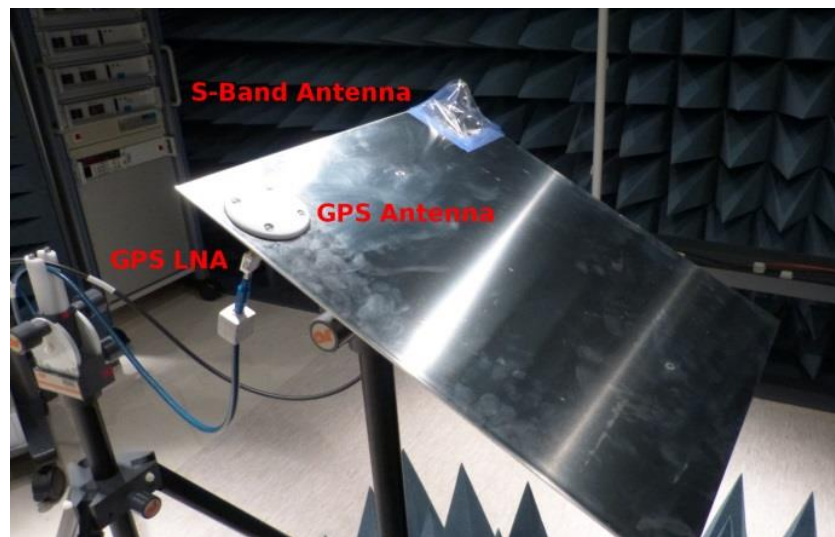


**Figure 5: GPS and S-Band Antenna Mounted on an Aluminum Plate for Interference Test**

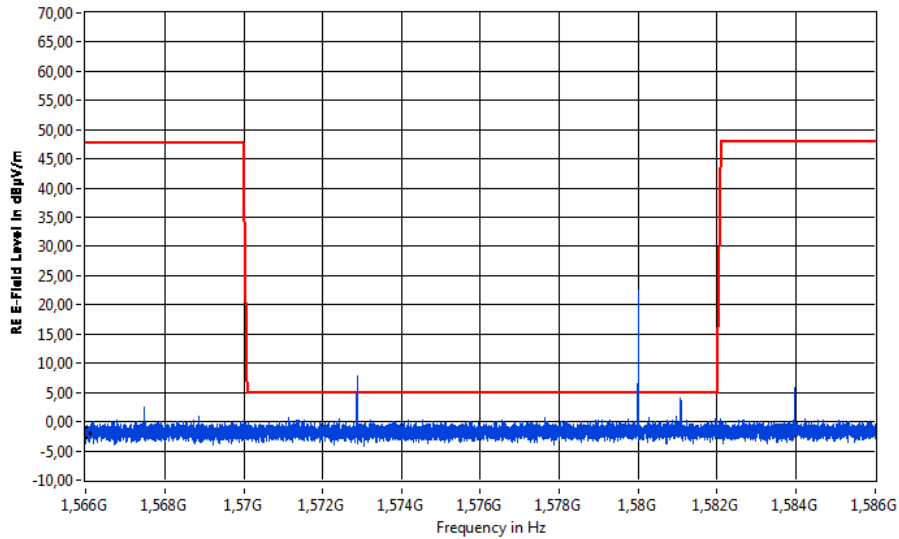


**Figure 6: Radiated Emission Notch Region and Results for GPS L1 (1.57 to 1.582 GHz)**

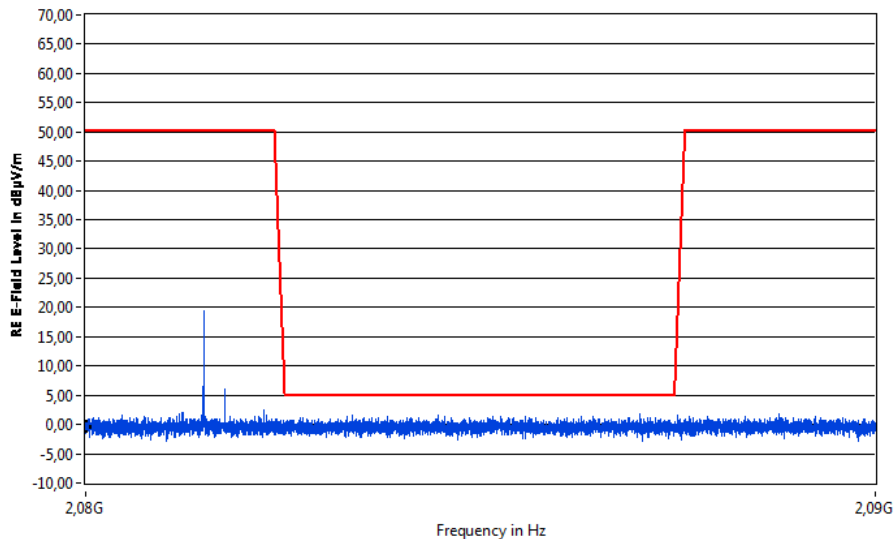


**Figure 7: Radiated Emission Notch Region and Results for Transmitter S-Band Uplink Frequency**

### VIBRATION TESTS AT ZARM

The vibration test of the complete spacecraft was executed at the ZARM Institute in Bremen, Germany. This test should verify the sufficient resistance of the spacecraft against mechanical loads occurring during the launch phase. Furthermore, the dynamic characteristics of the satellite should be measured in order to prove the compliance with the requirement of the first fundamental frequency for the launch provider.

#### *Vibration Test Definition*

Two possible launch systems were taken into account for the in-orbit transportation of the Flying Laptop at

the time of the vibration test. The first rocket was the Indian PSLV launching from Sriharikota. As a second launch option the Russian Soyuz Fregat was foreseen. The vibration test of the Flying Laptop was executed in a way that the requirements of both rockets were verified.

All flight components of the Flying Laptop were mechanically tested under qualification or acceptance loads. The main structure of the satellite was verified within a Structure and Thermal Model (STM) test that proved the mechanical characteristics by applying the qualification loads of the Soyuz launcher. Furthermore, the test results were used for the validation of the

mechanical and thermal simulations of the satellite (ref. 3). In order to measure the mechanical behavior of the STM acceleration sensors (13 three-axis and 3 one-axis sensors) were positioned all over the spacecraft. Besides the mechanical qualification of the satellite structure, this test defined the loads of the separate component vibration tests. Due to this previous mechanical verification of components and structure, the satellite flight model was tested under acceptance loads given by the launch provider.

Both launch providers expected a sine test and a random vibration test in each satellite axis for the vibration acceptance of the spacecraft. The sine test of the Soyuz Fregat is performed between 1 Hz and 20 Hz. However, if natural frequencies of the spacecraft exceed 40 Hz, it is allowed to omit sine tests at frequencies up to 20 Hz (ref. 4). Due to the STM results with a fundamental frequency at 65 Hz only the sine levels of the PSLV were tested (Table 1). The random vibration test levels were defined as a combination of PSLV and Soyuz requirements (Table 2 and Figure 8).

**Table 1: Sine Vibration Test Levels (ref. 5)**

	Frequency Range (Hz)	Test Level
Longitudinal axis (y-axis)	5 – 8	23 mm (double amplitude)
	8 – 100	3.0 g
Lateral axis (x- and z-axis)	5 – 8	16 mm (DA) (double amplitude)
	8 – 100	2.0 g
Sweep rate	4 Oct/min.	

**Table 2: Random Vibration Test Level (ref. 5 & 6)**

Frequency (Hz)	PSD (g <sup>2</sup> /Hz)
20	0.005
50	0.005
100	0.01
200	0.025
500	0.025
750	0.015
1000	0.015
2000	0.005
<b>total</b>	<b>5.2 grms</b>
Duration: 2 min	

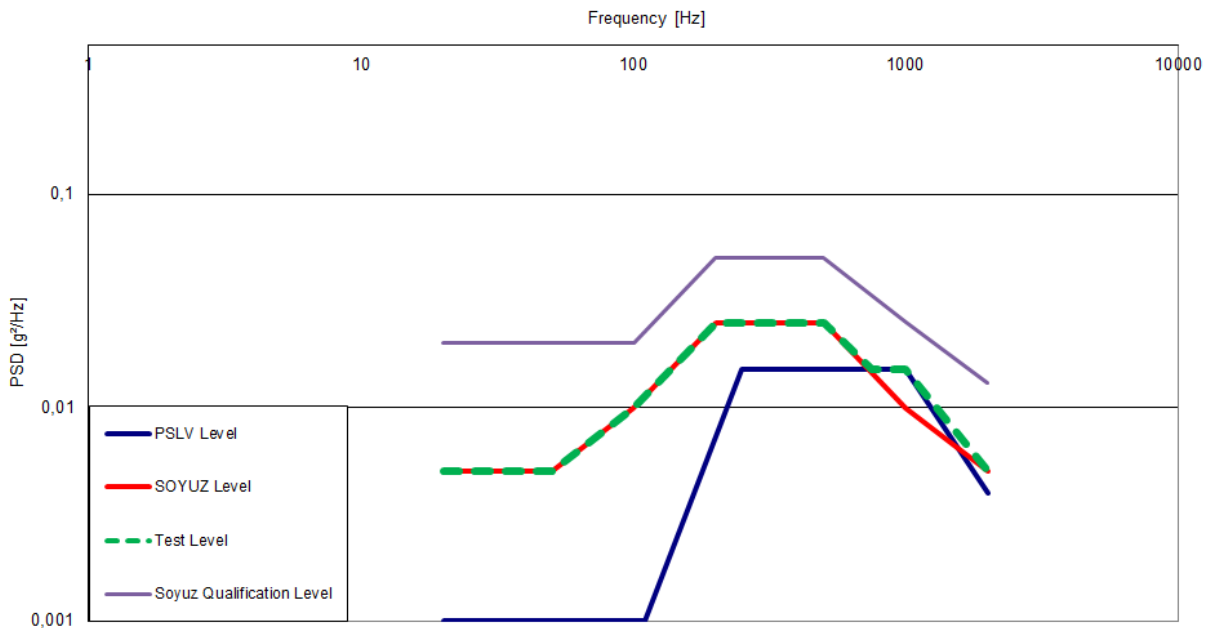


**Figure 8: Random Vibration Level of Test Combined from Launcher Levels**

The vibration behavior of the satellite and its critical components was observed by acceleration sensors installed in the spacecraft. The infrastructure of ZARM offered the implementation of 12 one-axis acceleration sensors. They were placed at critical positions that showed high response behavior during the STM test. Six positions were monitored during the test - 3 with one-axis and 3 with three-axis measurement (Figure 9).

In order to protect the components against unacceptable response loads, notching as well as abort criteria were defined. One of these criteria results from the component vibration test of the on-board computer

(OBC). The maximum random vibration level had to be notched at a certain frequency range in z-direction during the acceptance component test in order to protect the on-board computer from overloading. This notching spectrum (Figure 10) shall not be exceeded during the vibration test. Furthermore, a maximum load criterion of 15 g was established for the protection of the flight hardware. This means if a load higher than 15 g for sine and 15 grms for random vibration tests occurs at an acceleration sensor, the test levels shall be regulated or the test shall be aborted and a notching shall be implemented.

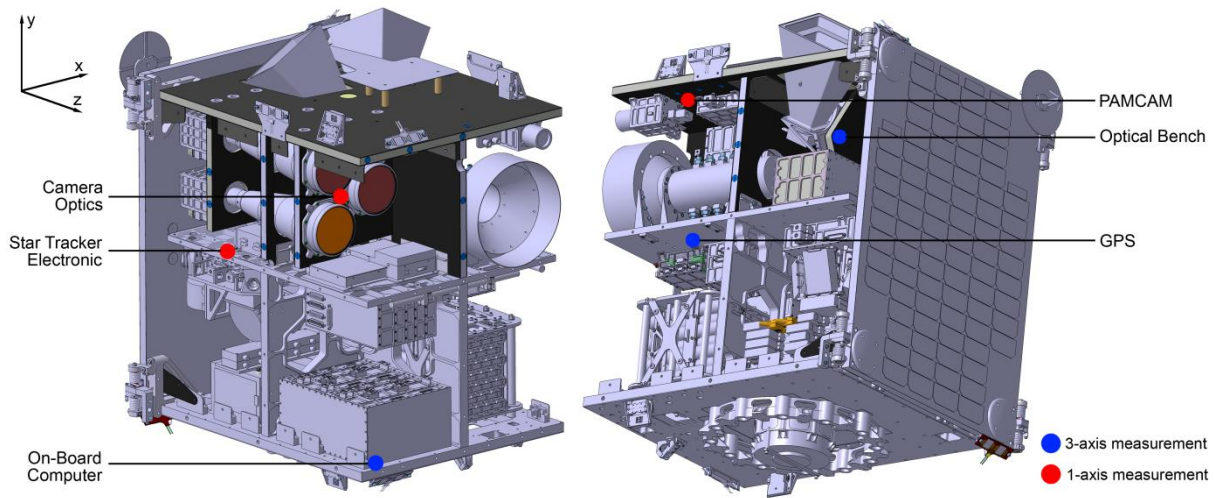


**Figure 9: Sensor Positions during Vibration Test**

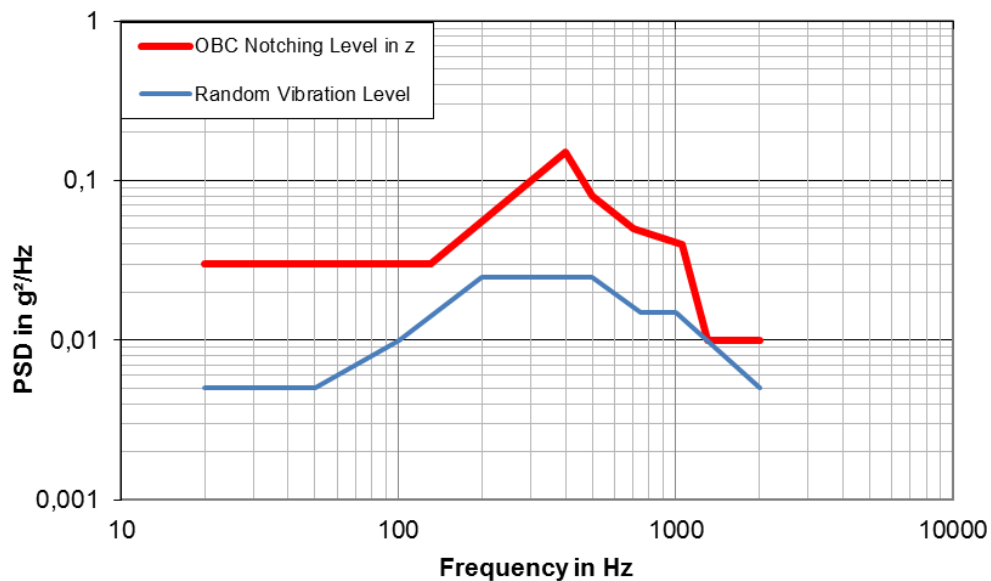


**Figure 10: On-Board Computer Notching Criterion in z-Axis**

The vibration test for Flying Laptop was conducted on a LDS V875 HBT 600 vibration test facility at the ZARM Institute. The shaker (Figure 11) is equipped with a slip table and exhibits the following characteristics:

- Frequency range: 5 - 3000 Hz
- Max. load: 600 kg (vertical operation)  
5000 kg (horizontal operation)
- Max. force vector: 35.6 kN sine and random,  
106.8 kN shock
- Max. acceleration: 110  $g_0$  (amplitude)
- Max. velocity: 1.8 m/s (amplitude)
- Max. stroke: 25.4 mm (amplitude)
- Mounting interface:  $\phi 440$  mm (armature)  
600x 600 mm<sup>2</sup> (head expander)  
600x700 mm<sup>2</sup> (slip table)

The vibration test was conducted in November 2014 over the period of one week. From Monday to Tuesday morning the satellite was prepared for testing. In order to exclude transport damages an abbreviated functional test was performed. Furthermore, the integration of the accelerometers was done in a ISO 7 clean room at the ZARM Institute. On Tuesday afternoon the satellite was mounted to the horizontal slip table and the vibration test was carried out for the x-axis. The tests in the z-

and y-axis followed on Wednesday. The z-axis was also tested on the horizontal slip table and the y-axis test was executed in the vertical direction after a rotation of the shaker head by 90°. During the tests a foil tent was used to protect the satellite against dust and other contamination during the shaker tests inside the ZARM Vibration Test Lab (Figure 12). On Thursday and Friday the vibration tests were finished with the abbreviated functional check, the disintegration of the acceleration sensors, and the preparation for transport.

The test procedure of the vibration test for each axis is shown in Table 3. The test of each axis started with a sine resonance search with low load. With this test the dynamic frequency behavior of the spacecraft can be measured for each axis. After each mechanical acceptance test this sine resonance search was repeated in order to identify structural damages that would change the dynamic behavior of the spacecraft. As first acceptance test the sine vibration test was executed. Due to the automatic abort criterion of 15 g this test was conducted with full load. Such an abort criterion could not be set during the random test. Thus, a pre-test with -12 dB of the load (approximately one fourth of the full load) was conducted in order to estimate the occurring load during the following full level random test.



**Figure 11: ZARM Shaker Facility**



**Figure 12: Vibration Test Protected by a Tent**

### Vibration Test Result

The first sine resonance searches of all axes revealed the frequency-dependent dynamic behavior of the spacecraft and the amplification generated by the excitation load. By means of this test the fulfilment of the first fundamental frequency requirement of the launchers could be verified. The first eigenfrequencies of the respective satellite axis and their amplifications are shown in Table 4. Furthermore, the sine resonance tests result in a high amplification factor below 100 Hz. The frequency behaviour in the satellite's x-axis is shown in Figure 13. The first eigenfrequency of the satellite corresponds well with the results of the structural finite element simulation predicting a first eigenfrequency of 72 Hz.

All sine vibration tests were executed without causing visual damages. However, the 15 g criterion was exceeded in x- and z-direction. In each case the excitation load was reduced in a way that the acceleration sensor of the optical bench (CHU) stays below 15 g. Thus, the excitation load was decreased to a minimum of 1.2 g in the x-axis and to a minimum of 0.6 g in the z-axis in the region of resonance. Due to the high resonance frequencies of the y-axis, notching of this axis was not necessary. Figure 14 shows the test results of the sine vibration test in the z-axis.

Like the sine vibration tests all random vibration tests were carried out without visual damages. The x-axis could be performed without notching. The notching criterion of the on-board computer (Figure 10) was

minimally breached during the random vibration test in z-direction, so the excitation was regulated around 1100 Hz during the test. The overall load was reduced by 0.016 grms from the specified value. A higher modification of the excitation was necessary during the random tests in y-direction. The estimation from the random vibration pre-test showed an unacceptable load at the position of the panorama camera PAMCAM in the region of its first resonance frequency. Thus, in the region of 200 Hz to 300 Hz the excitation load was reduced (Figure 15). With this notching the overall load was reduced by 0.13 grms from the specified value. Due to this notching the PAMCAM acceleration sensor measured a load of 17.3 grms during this test.

At the end of each vibration test the results from the sine resonance searches were compared. This showed some small deviations in frequency and amplitude. These are results of settling of joint tensions that were generated by the assembly of the satellite components. Due to vibration loads these tensions were reduced and changed the dynamic behavior of the spacecraft. However, the deviation did not exceed the required frequency shift of 5 %. In Figure 16 the results from the three y-axis sine resonance searches of the highly loaded PAMCAM acceleration sensor are illustrated.

After the vibration test the satellite's integrity was checked by the abbreviated functional tests. All satellite systems showed correct performance, thus the vibration test was completed successfully.

**Table 3: Test Procedure for each Axis**

No.	Test
1	Sine Resonance Search 5-2000 Hz; 0.2 g; 2 Oct./min
2	Sine Vibration Test Table 1
3	Sine Resonance Search 5-2000 Hz; 0.2 g; 2 Oct./min
4	Random Vibration Pre-Test (-12 dB level) Table 2
5	Random Vibration Test (full level) Table 2
6	Sine Resonance Search 5-2000 Hz; 0.2 g; 2 Oct./min

**Table 4: First Eigenfrequencies of Flying Laptop**

Axis	First eigenfrequency	Amplification factor of load
x	75 Hz	21
y	No distinct one (local 267 Hz)	- (33)
z	78 Hz	32

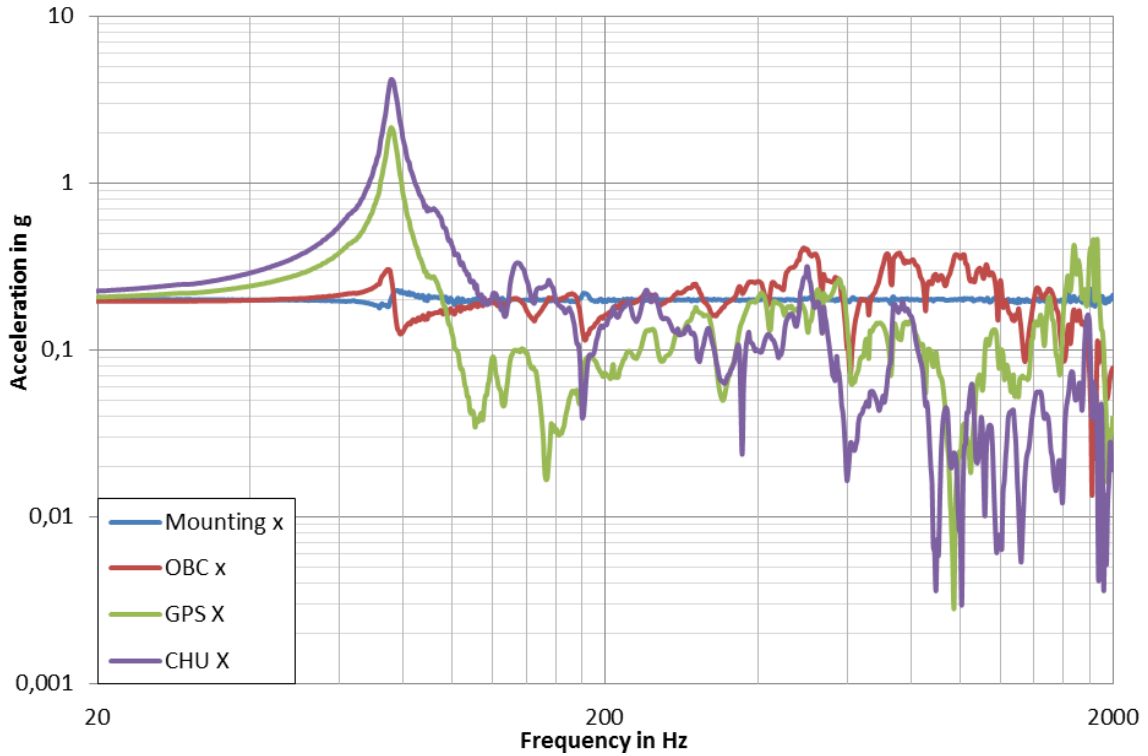


**Figure 13: Satellite Response during First Sine Resonance Search in x-Axis**

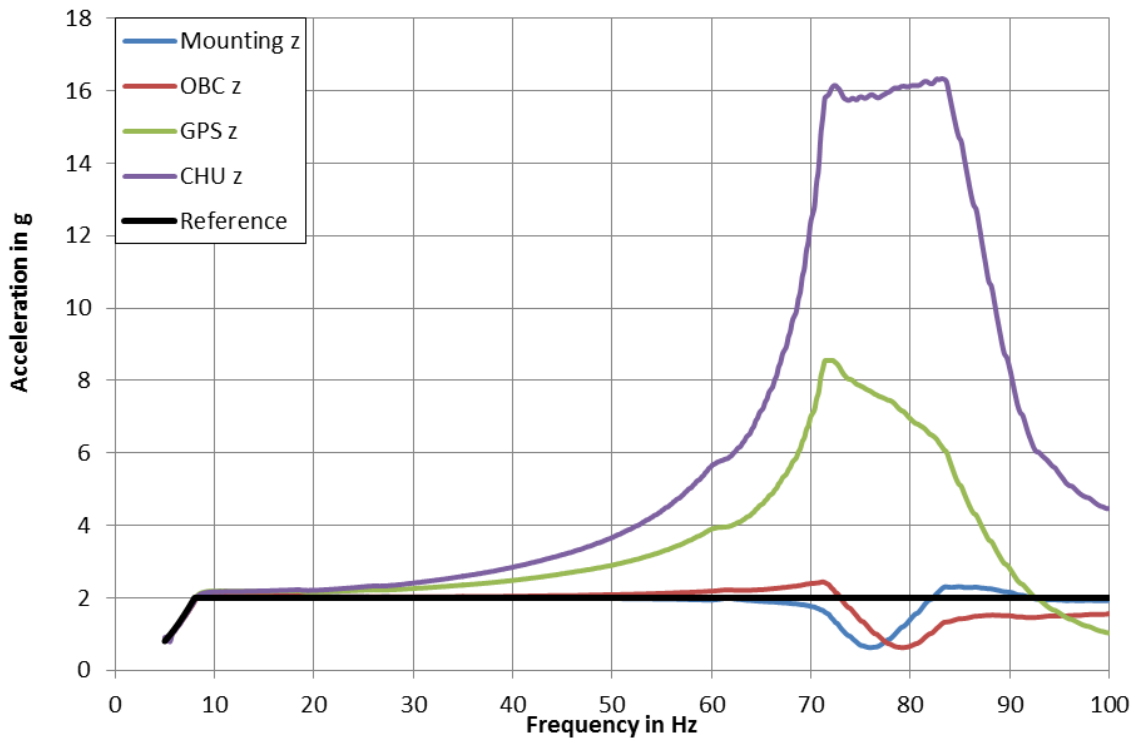


**Figure 14: Sine Vibration Test of z-Axis**

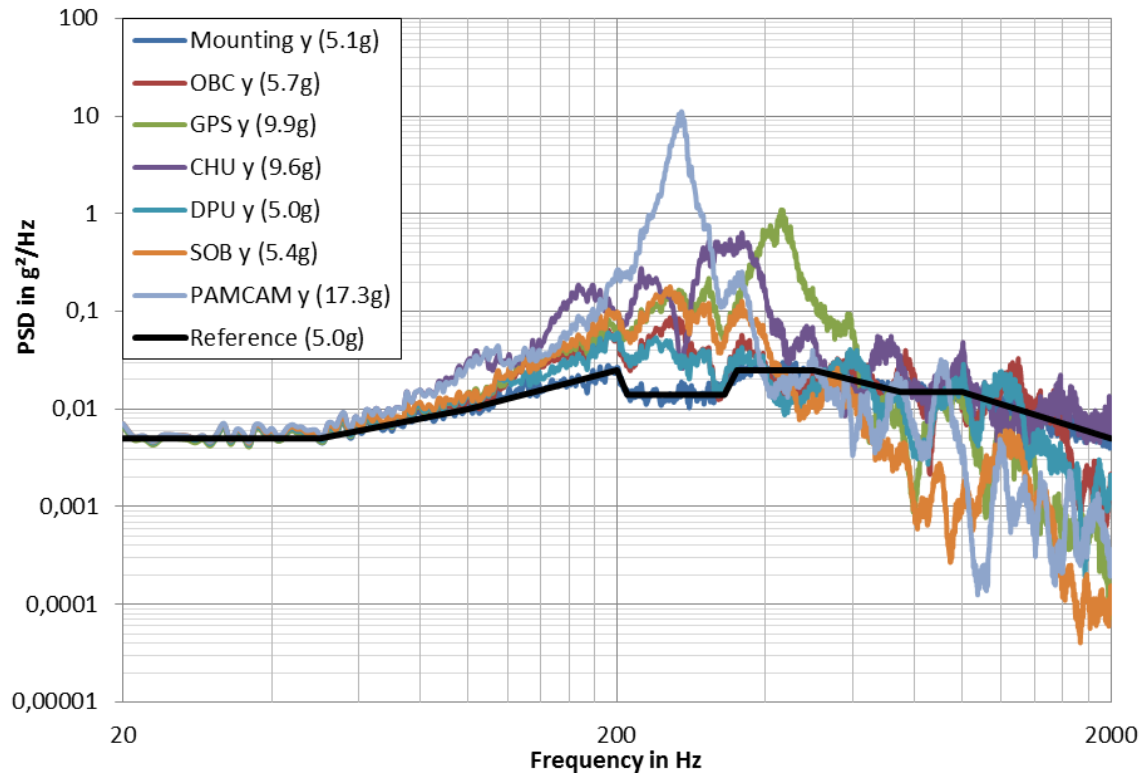


**Figure 15: Response Spectrum of Random Vibration Test of y-Axis**

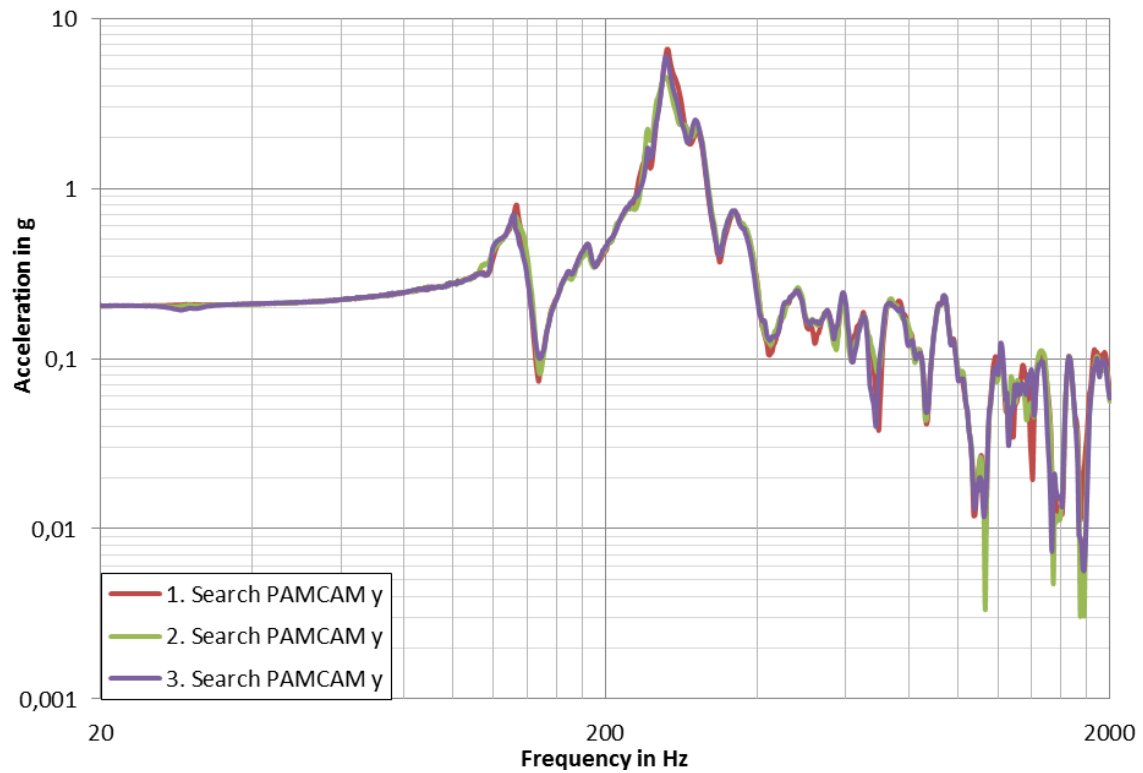


**Figure 16: Overlaid Sine Resonance Searches of y-Axis Test at PAMCAM Position**

## THERMAL TEST AT DLR

The thermal test was conducted at DLR in Berlin-Adlershof, Germany. As part of the environmental tests for the flight model of the Flying Laptop, the satellite with all components was to demonstrate full functionality in vacuum while being operated under hot and cold extreme temperature conditions. Subsequently, a thermal balance test was to be performed. With the results of this test the satellite's thermal model would be validated by fitting the calculated temperatures to the measurements. As both of these tests pose different requirements to the test setup, the test environment is explained in the following section. This is followed by the description of the actual tests and their results.

### *Thermal Test Definition*

The vacuum chamber at the DLR in Berlin, Germany, offers the volume to accommodate the entire satellite as well as the ability to simulate a cold environment using a shroud fed with liquid nitrogen. The chamber with the satellite can be seen in Figure 17. The facility also offers sun simulation with a limited beam size, which was too small for the Flying Laptop. The details on the thermal vacuum chamber can be found in Table 5.

In order to outline a test setup, the test goals need to be properly defined. The purpose of the thermal test can be summed up in the following two points:

1. Verification of the system operability at the expected low and high temperatures,
2. Validation of the thermal model.

For point 1, the verification, a full representation of the radiative environment is not necessary as long as the satellite and its components are subject to the desired temperature levels. For point 2 a representation of the radiative environment is desirable in order to reduce

deviations in the thermal model. Having set these test goals, different tests setups were evaluated as summarized in Table 6.

The chosen test setup was a mixture of two methods. For the verification of the system functionality (test goal no. 1) the satellite is mounted to a temperature controlled metal plate via a thermally conductive interface. The validation of the thermal model (test goal no. 2) is achieved with the same setup of temperature controlled plates, but the interface is replaced with a thermal insulation. Due to the usage of a conductive interface test time and cost could be reduced. The different interfaces are shown in Figure 18 and Figure 19.

This means that the vacuum test is split up into two parts:

1. A thermal vacuum test for the system verification.
2. A thermal balance test for the validation of the thermal model.

In-between the two tests the vacuum chamber was opened and the mounting interface was changed from conductive to insulated.

Additional metal plates were heated / cooled during the thermal balance test in order to simulate the orbital heat flux input on the satellite's surface. Since the heat flux through the multi-layer insulation is rather small, there were only metal plates in front of the satellite's radiators and solar panels. The entire setup for controlling the satellite's environment is depicted in Figure 20 and Figure 21. The metal plates were equipped with electrical heaters and had a black coating (Aeroglaze Z307) to increase the infrared emissivity.

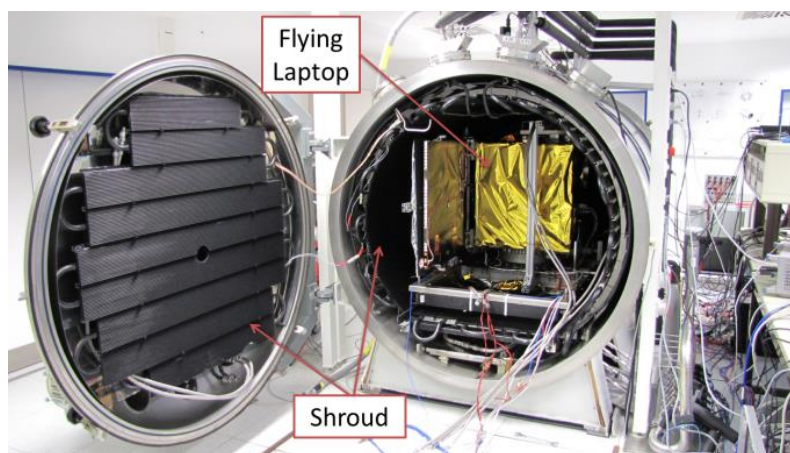


**Figure 17: The Flying Laptop inside the Thermal Vacuum Chamber**

**Table 5: Thermal Vacuum Test Facility at DLR Berlin**

Parameter	Value
Pressure level	$1.33 \times 10^{-5}$ mbar
Shroud temperature	80 K (liquid nitrogen)
Shroud dimensions	$\varnothing 1300 \text{ mm} \times 2500 \text{ mm}$
Usable volume	3.2 m <sup>3</sup>
Sun simulation	0...2.8 kWm <sup>2</sup> on $\varnothing 300 \text{ mm}$
Sun spectrum	0.2...2.5 $\mu\text{m}$
Beam divergence	10° - 15°
Beam homogeneity	65%

**Table 6: Test Setup Comparison**

Environment		Pros	Cons
Heat transfer via radiation	Sun simulator	Validation of optical properties at begin of life	Expensive, beam too small
	Infrared lamps	Very high heat flux density possible	Homogeneous illumination difficult, no visible spectrum
	Temperature controlled metal plates/sheets as infrared radiator (ref. 7)	Environmental conditions well known, can be used as heat sink	No visible spectrum
Heat transfer via conduction	Heaters mounted directly to the spacecraft (ref. 8)	Cost effective method	No validation of optical properties
	Temperature controlled metal plate connected via conductive interface	Hot and cold temperatures possible	Thermal balance test not reasonable

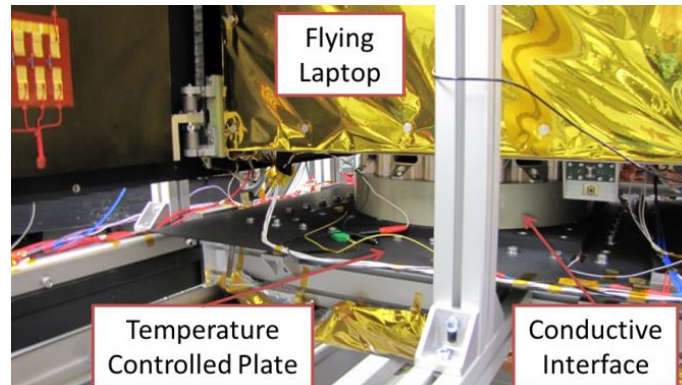


**Figure 18: Conductive Mounting Interface (Massive Aluminum Flange) during Thermal Vacuum Test**

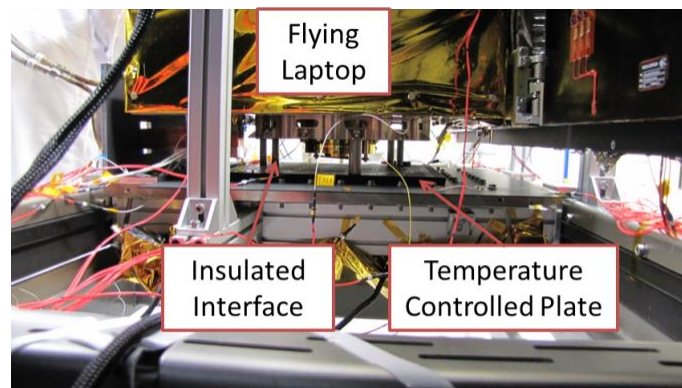


**Figure 19: Insulated Mounting Interface (6 PEEK Bushes) during Thermal Balance Test**

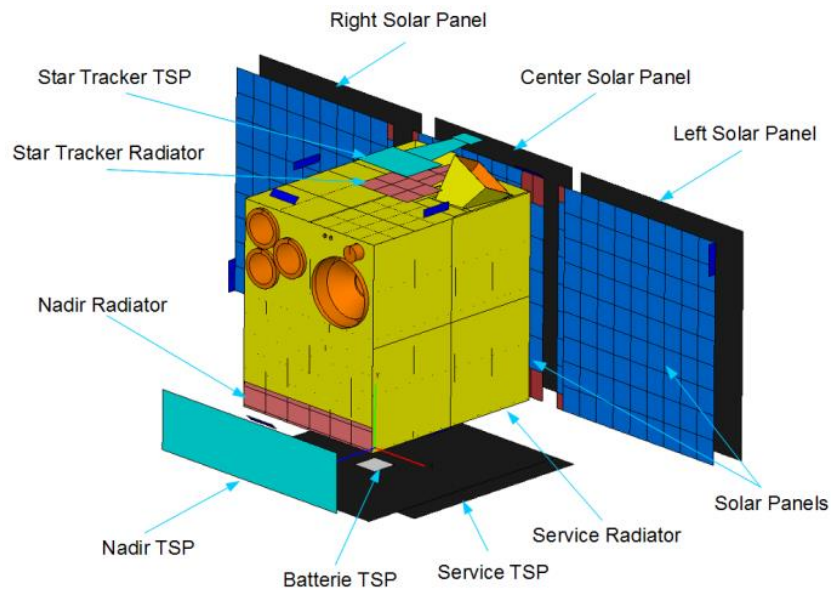


**Figure 20: Temperature Controlled Metal Plates (TSP) for Regulation of the Satellite's Environment**

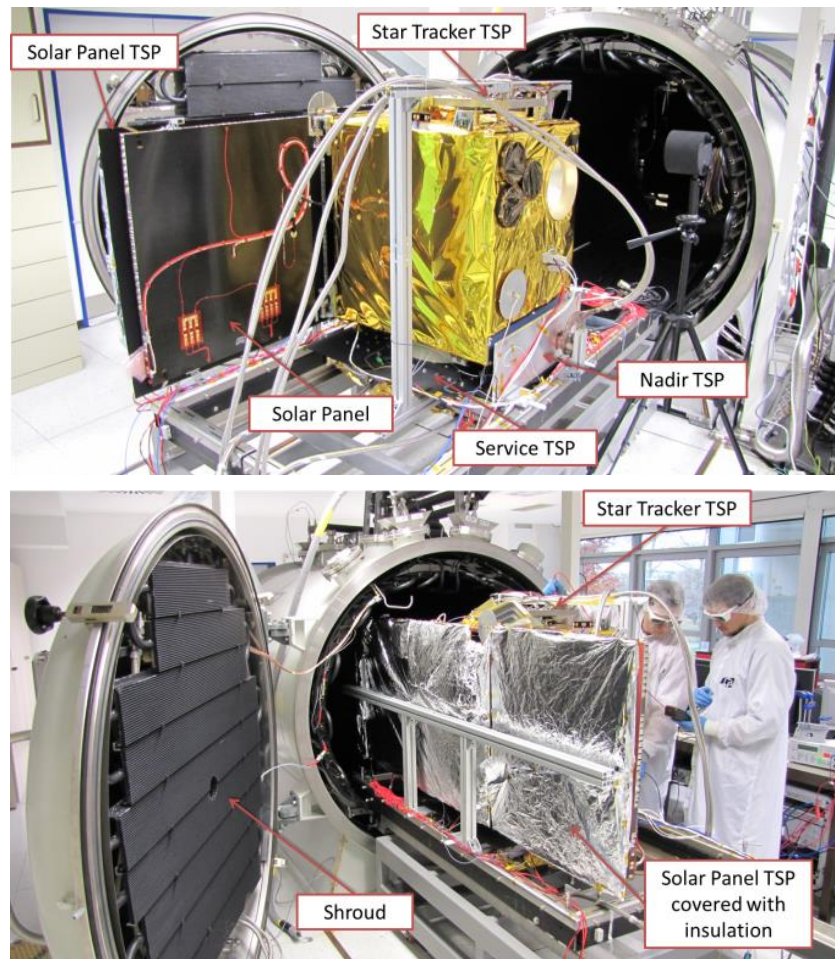


**Figure 21: The Final Test Assembly before Closing the Chamber**

During the thermal balance tests the satellite shall have similar surface temperatures as in orbit. Therefore, the method for calculating the temperature of each plate is explained in the following. A preliminary temperature of each metal plate is derived from an analytical correlation (see also ref. 9 and ref. 10). The correlation uses the assumption of the heat transfer between two infinite parallel plates with multi-reflexion. The occurring heat fluxes are shown in Figure 22.

With this assumption, the following equation can be derived:

$$T_{Pl} = \left( ((\dot{q}_S + \dot{q}_A + \dot{q}_E)A - \sigma A \varepsilon T_{Sat}^4) \frac{1}{\sigma \cdot GR} + T_{Sat}^4 \right)^{1/4}$$

where  $T_{Pl}$  = temperature of the metal plate (K);

$\dot{q}_S + \dot{q}_A + \dot{q}_E$  = absorbed heat flux of solar, albedo and earth radiation (W/m<sup>2</sup>);

$A$  = irradiated surface area (m<sup>2</sup>);

$\sigma$  = Stefan-Boltzmann constant (W/m<sup>2</sup>K<sup>4</sup>);

$\varepsilon$  = infrared emissivity of the sat. surface (-);

$GR$  = effective radiative conductor between metal plate and satellite surface (-);

$T_{Sat}$  = surface temperature of the satellite (K).

The basis of this correlation is a uniform radiative heat flux on the satellite surface. The used heat flux is derived from a stationary orbit simulation. Therefore the heat flux is the average flux over one orbit. The correlation can be used as long as  $\dot{q}_S + \dot{q}_A + \dot{q}_E > \sigma A \varepsilon T_{Sat}^4$  is valid.

The resulting preliminary temperatures are used as input for the thermal simulation of the chamber setup. With a manual iteration for the plate temperatures the satellite surface temperature is matched between orbit and chamber simulation. The result of this iteration is summed up in Table 7. The resulting heat flux differs from the orbit values due to the multi-reflexion. This fact is shown in Table 8.

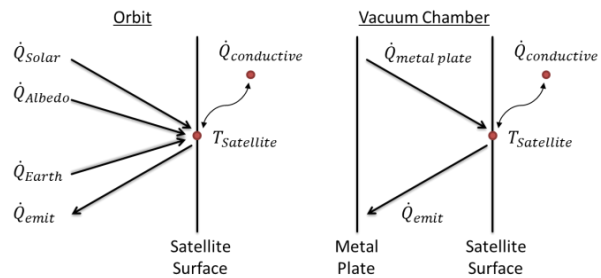


**Figure 22: Model for the Analytical Correlation**

**Table 7: Calculated Surface Temperature for Orbit and Thermal Vacuum Chamber Simulation**

Surface	Hot Case (°C)		Cold Case (°C)	
	Orbit	Test	Orbit	Test
Center Solar Panel	97.7	97.9	87.2	87.2
Left Solar Panel	83.5	83.5	71.2	71.1
Right Solar Panel	83.6	83.6	71.2	71.3
Battery Radiator	35.4	35.3	25.0	24.9
Nadir Radiator	31.6	27.9	-14.9	-17.4
Service Radiator	27.1	27.6	-17.5	-17.5
Star Tracker Radiator	-73.1	-73.1	-70.5	-70.5

**Table 8: Calculated Absorbed Heat Flux for Orbit and Thermal Vacuum Chamber Simulation**

Surface	Hot Case (Watt)		Cold Case (Watt)	
	Orbit	Test	Orbit	Test
Center Solar Panel	339.2	315.3	302.3	281.3
Left Solar Panel	403.1	386.9	360.1	340.5
Right Solar Panel	403.1	388.5	360.1	341.5
Battery Radiator	0.14	0.1	0.07	0.04
Nadir Radiator	6.5	3.0	1.9	2.7
Service Radiator	19.6	18.2	9.8	5.8
Star Tracker Radiator	19.6	18.2	9.8	5.8

### Thermal Test Results

The thermal tests were successfully conducted and all the goals were achieved. The entire thermal profile can be seen in Figure 23. During the verification of the system the satellite's main bus components reached temperatures from -20 °C to +40 °C. The payload was operated successfully from 0 °C to +40 °C. Abbreviated functional tests were performed for every component in order to verify their functionality at the extreme temperature conditions. An exemplary temperature curve of the on-board computer can be seen in Figure 24.

In two cases with different environmental conditions during the thermal balance test the satellite reached temperature stability according to the following criterion:

$$|T_{average\ 1h}(t) - T_{average\ 1h}(-5\ h)| < 0.5\ K$$

where  $T_{average\ 1h}(now)$  = temperature averaged over 1 hour, using the latest measurement values;

$T_{average\ 1h}(-5\ h)$  = temperature averaged over 1 hour, using values measured 5 hours before.

The advantage of using averages instead of the temperature gradient is the stability against oscillations in the temperature curve due to sensor noise or the transient control deviation of the environmental temperatures. As an example the steady state can be seen in Figure 25, showing the temperature curve of the receiver for the maritime ship signal AIS. After the hot case balance test the entire payload was successfully operated for 20 minutes, resulting in a maximum temperature increase of +5 K at the temperature reference points of every payload. This means that the satellite can withstand short term increased power dissipation from about 50 Watts (standard mode) to more than 150 Watts (all payloads on).

The measured temperatures were used to validate the thermal model. After the adaptation of several model parameters all sensor values matched the measured values in both cases with a maximum deviation of  $\pm 5$  °C. Figure 26 shows the distribution of the temperature differences (measured value minus calculated value).

The corresponding global temperature deviation is:

$$\Delta T = \frac{1}{N} \sum_{i=1}^N (T_{M_i} - T_{P_i})$$

Hot Case:  $\Delta T = -0.5\ K$

Cold Case:  $\Delta T = -0.3\ K$

The standard deviation is:

$$\sigma = \frac{1}{N-1} \sqrt{\sum_{i=1}^N ((T_{M_i} - T_{P_i}) - \Delta T)^2}$$

Hot Case:  $\sigma = 1.9\ K$

Cold Case:  $\sigma = 1.6\ K$

where  $\Delta T$  = global temperature deviation (K);

$N$  = number of temperature measurements considered for correlation (hot case: 51, cold case: 48);

$T_{M_i}$  = measured temperature (K);

$T_{P_i}$  = calculated temperature (K);

$\sigma$  = standard deviation of all temperature differences (K).

The precision of the results were considered to be sufficient to predict the satellite's behavior in orbit.

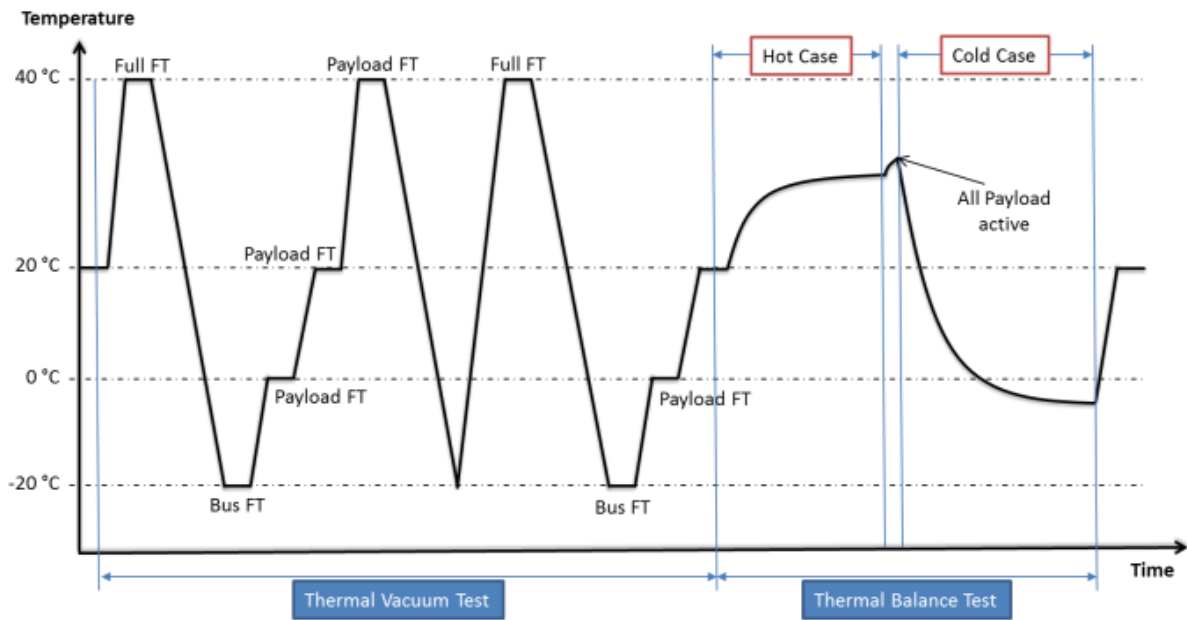


Figure 23: Temperature Profile for the Vacuum Test (FT: Functional Test)

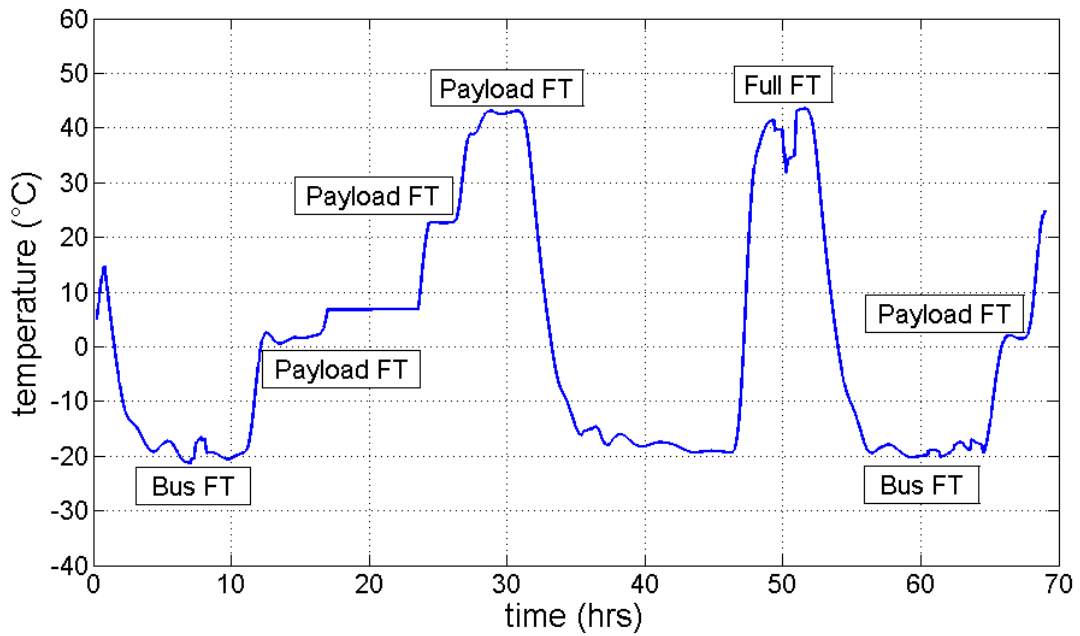


Figure 24: Temperature Curve of the Temperature Sensor at the On-Board Computer during the Thermal Vacuum Test (FT: Functional Test)

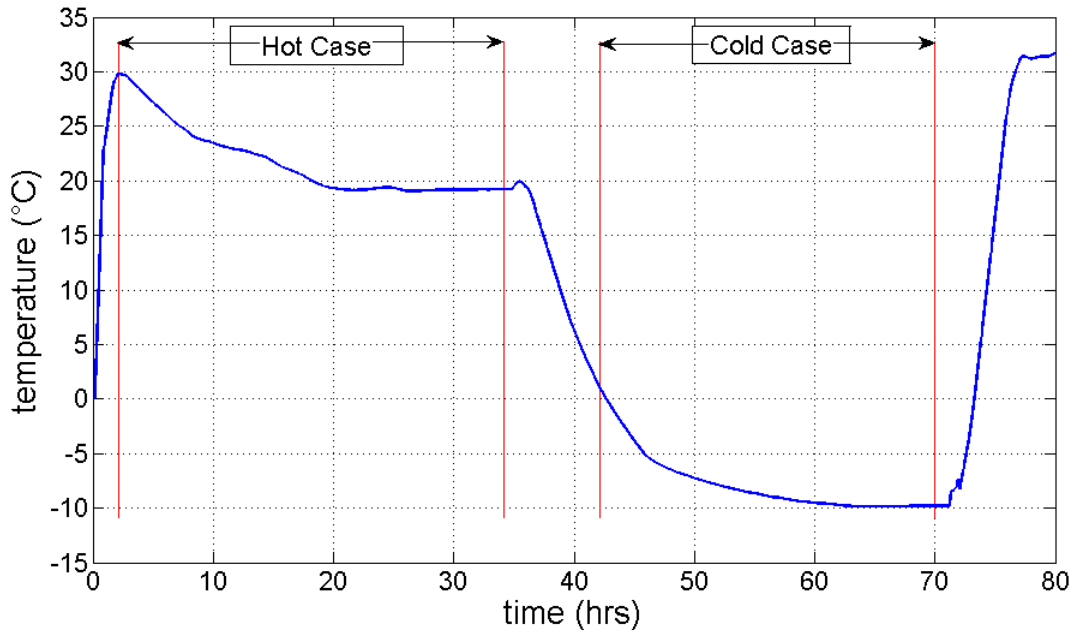


Figure 25: Temperature Curve of the AIS Receiver Payload during the Thermal Balance Test

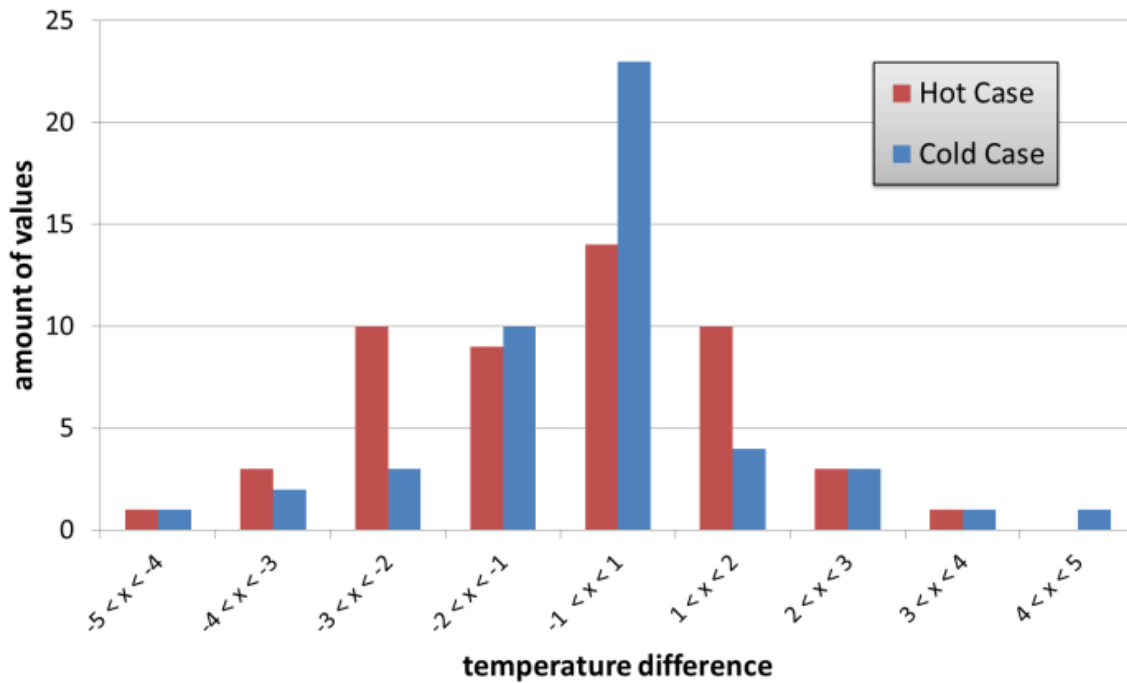


Figure 26: Temperature Differences between Measurement and Simulation - Measured Value Minus Calculated Value (ref. 11)

## CONCLUSION

The environmental acceptance tests were successfully conducted on the flight model of the small satellite Flying Laptop. All requirements were met and the satellite behaved as expected.

The satellite on-board components proved to be electromagnetically compatible and the amount of crosstalk of the internal harness is below critical levels. No significant interference between the radio-frequency systems was found.

Furthermore, the satellite structure was verified to survive the mechanical loads occurring during satellite launch. The applied test loads resulted from a combination of two possible launcher requirements, providing scope for launch negotiations. The vibration test was conducted successfully without any events or damages.

During the thermal vacuum test the satellite demonstrated its functionality in the temperature range from -20 °C to +40 °C and included the payload operation in the desired temperature range from 0 °C to +40 °C. The temperature measurements were successfully transferred to the thermal model in order to reliably predict the behavior in orbit.

With these tests the satellite has proven to withstand the environmental conditions during launch and in orbit. Therefore, following the subsequent functional system tests, the satellite will be ready to launch.

## ACKNOWLEDGMENTS

The realization of the Flying Laptop project was only possible due to the support of many individuals and organizations. Therefore, the Flying Laptop team would like to express its sincere gratitude to all of them.

For the support of the environmental test campaign the Flying Laptop team is deeply grateful to Airbus Defence and Space, DLR Bremen, DLR Berlin, as well as the ZARM Institute for providing their expertise, technical support, and facilities for test definition and conduction. Without this help the campaign would not be carried out in this effective and successful way. Especially for the financial support very special thanks go to Airbus Defence and Space and DLR Bremen.

The Flying Laptop team would like to express sincere thanks towards all the students who devoted their time and knowledge for preparation and conduction of the environmental test campaign.

## ABBREVIATIONS AND ACRONYMS

AIS	Automatic Identification System
DLR	German Aerospace Center (Deutsches Zentrum für Luft- und Raumfahrt)
EMC	Electromagnetic Compatibility
GPS	Global Positioning System
PEEK	Polyether Ether Ketone
PSLV	Polar Satellite Launch Vehicle
STM	Structure and Thermal Model
ZARM	Center of Applied Space Technology and Microgravity in Bremen, Germany

## REFERENCES

1. ESA, DLR, CNES, ASI, BNSC, “European Code of Conduct for Space Debris Mitigation”, 2004.
2. Jean, C., “Charakterisierung der FLP Satellitenplattform hinsichtlich elektromagnetischer Verträglichkeit“, Bachelor Thesis, Hochschule Mannheim, 2014.
3. Steinmetz, F. et al., ”Validation of the Structural-Thermal Model of the Small Earth Observation Satellite Flying Laptop”, Small satellites for earth observation: 9th IAA symposium, Berlin, 2013.
4. ECM Launch Service, “Loading environment for small SC (secondary payloads)”, 2014.
5. Ramakrishnan, S., “PSLV - Auxiliary Satellite User’s Manual”, Issue 1, Indian Space Research Organisation, 1999.
6. Perez, E., “Soyuz User’s Manual”, Issue 2, Ariane Space, March 2012.
7. Almeida, J. S. et al., “Effectiveness of low-cost thermal vacuum tests of a micro-satellite”, Acta Astronautica, Vol. 59, p. 483–489, 2006.
8. Garcia, E. C. et al., “Space Simulation of the China-Brazil Earth Resources Satellite CBERS”, Revista de Engenharia Térmica, Vol. 3, Nr. 2, p. 100–106, 2004.
9. Maurer, P., “Preparation of the Thermal Vacuum Tests for the small satellite Flying Laptop”, Bachelor Thesis, University of Stuttgart, 2015.
10. Yang, K. et al., “Development of the GPM Observatory Thermal Vacuum Test Model”, Thermal and Fluids Analysis Workshop 2012 Proceedings, Pasadena, California, 2012.
11. Steinborm, D., “Validation of the Flying Laptop Thermal Model by Thermal-Vacuum Tests”, Master Thesis, University of Stuttgart, 2015.